Equilibrium Theory Analysis of Dual Reflux PSA for Separation of a Binary Mixture

Armin D. Ebner and James A. Ritter
Dept. of Chemical Engineering, Swearingen Engineering Center, University of South Carolina, Columbia, SC 29208

DOI 10.1002/aic.10191
Published online in Wiley InterScience (www.interscience.wiley.com).

A dual reflux (DR) PSA cycle that combines the features of a conventional (stripping reflux) PSA cycle with those of a new enriching reflux PSA cycle is analyzed to show its potential for separating gas mixtures. On the basis of isothermal equilibrium theory applied to linear isotherms, the ultimate separation is carried out where the binary feed is separated into two pure components with 100% recovery of each component. This very idealized analysis reveals that such a separation is possible over a wide range of conditions, even with pressure ratios as low as 1.1. This analysis also reveals that low throughputs and high heavy component recycle ratios are inherently associated with DR PSA cycles, both of which may be detrimental to the process economics. High throughputs and low heavy product recycle ratios are indeed achievable, but only when using low pressure ratios and less selective adsorbents, both counterintuitive results that make sense when considering the perfect separation is always being achieved. Although these trends may not carry over to actual practice, because the model developed here is overly simplified and invalid under certain conditions, this analysis shows that it may indeed be entirely feasible to separate a binary gas mixture into two relatively pure components with very high recoveries using a DR PSA cycle operating with a very low pressure ratio and, hence, expenditure of energy. © 2004 American Institute of Chemical Engineers *AIChE J,* 50: 2418–2429, 2004

Introduction

Pressure swing adsorption (PSA) has gained considerable commercial acceptance over the past three decades (Ruthven et al., 1994), with a wide variety of applications for gas separation and purification in use today. Because of its modus operandi, however, state of the art PSA has been limited mostly to the purification of the light component from bulk gas streams. Some exceptions exist, but they necessarily require a high heavy component feed concentration, large pressure ratios, complicated cycle sequences, or multiple trains of columns to produce a relatively pure heavy component or two components both in high purity. This is a direct consequence of the four basic cycle steps associated with the original or Skarstrom type cycle, which is utilized by most PSA processes. These four steps include a high-pressure adsorption or feed step, a countercurrent blowdown step, a countercurrent low-pressure purge step, and a pressurization step carried out with either cocurrent feed or countercurrent light product.

In theory, the Skarstrom cycle allows for the complete purification of the light component during the high-pressure feed step. However, during the low-pressure purge step, the enrichment of the heavy component is limited by the pressure ratio, a purely thermodynamic constraint (Subramanian and Ritter, 1997). Interestingly, this limitation vanishes if the pressures corresponding to the feed and purge steps of the Skarstrom cycle are reversed, that is, if the feed step is carried out at low-pressure and the purge step is carried out at high pressure. Diagne et al. (1994) mentioned that, in such a PSA process, the enrichment of the heavy component is no longer limited by the pressure ratio; this fact has been demonstrated theoretically by Ebner and Ritter (2002), and experimentally by Yoshida et al. (2003).

The consequence of these recent studies is the redefinition of

Correspondence concerning this article should be addressed to J. Ritter at ritter@engr.sc.edu.

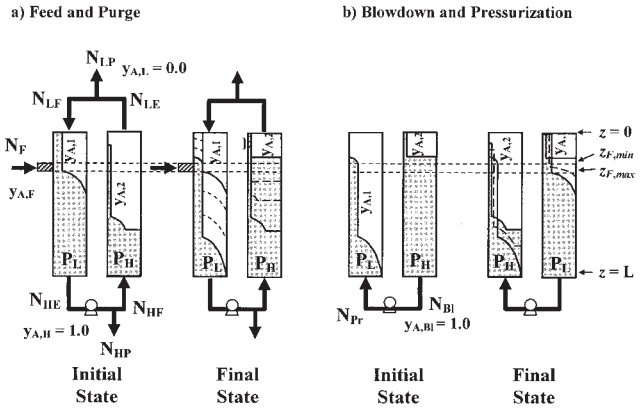

Figure 1. Initial and final concentration states (in gray) of the (a) two constant pressure steps (feed and purge), and (b) two pressure varying steps (pressurization and blowdown) that constitute the DR PSA cycle.

The feed and pressurization steps are depicted by the columns on the left in (a) and (b); and the purge and blowdown steps are depicted by the columns on the right in (a) and (b). The two horizontal (dashed) lines indicate the possible range of the feed location that ensures $y_{A,F} = y_{A,1}$ during the feed step.

PSA cycles as being either stripping or rectifying (also called enriching) by drawing a direct analogy with distillation. For example, to produce a pure light component a stripping reflux (SR) PSA cycle can be utilized, whereas, to produce a pure heavy component, an enriching reflux (ER) PSA cycle can be used. Clearly, it seems entirely plausible based on this analogy to combine the SR and ER PSA cycles together into a dual reflux (DR) PSA cycle. In fact, Diagne et al. (1994, 1995, 1996), McIntyre et al. (2002), and McIntyre and Ritter (2005) all showed that it is possible to configure a relatively simple DR PSA cycle, with light and heavy component enrichments only constrained by the mass balance, a feature of paramount importance. The extreme limit of a DR PSA system is the complete separation of a binary feed into two pure components, but this concept has never been demonstrated either experimentally or theoretically. Therefore, the objective of this work is to show theoretically that perfect separation is entirely feasible with a DR PSA cycle.

A twin-bed DR PSA cycle for separating a binary feed is formulated and analyzed according to isothermal, linear isotherm, equilibrium theory (Knaebel and Hill, 1985; Ebner and Ritter, 2002). Analytic expressions that describe the effects of all the important process parameters on the periodic state process performance are derived. These include expressions that show the effect of the pressure ratio, selectivity, feed concentration, and light product volumetric purge to feed ratio on the light and heavy recycles, heavy product volumetric purge to feed ratio, feed location, and productivity. A parametric study is also carried out over a wide range of conditions to demonstrate the utility of a DR PSA cycle for separating binary feeds into two pure products with 100% recovery of each component.

Cycle Description

Figure 1 depicts the twin-bed DR PSA system under consideration. This particular cycle (many other cycle configurations are possible) consists of two steps carried out simultaneously at constant pressure (Figure 1a), and two steps carried out simultaneously at varying pressure (Figure 1b). In each case, the twin-bed system on the left represents the cycle steps at the initial state, whereas the twin bed system on the right represents the cycle steps at the final state. During the cycle, N_F, N_{LF}, N_{HE}, N_{HF}, N_{LE}, N_{Pr} and N_{Bl} represent the total moles of gas leaving or entering the columns where indicated. The feed is located along the columns at some determinable location, and recycle loops are located at the ends of the columns. Each column undergoes the same four cycle steps: (1) a low, constant pressure step at P_L, (2) a countercurrent pressurization step from P_L to P_H, (3) a high, constant pressure step at P_H, and (4) a cocurrent depressurization, or blowdown step from P_H to P_L.

During step 1, the low-pressure column is essentially being fed with two feeds, N_F and N_{LF}. In this analysis N_{LF}, the light reflux, always enters the top of the column as it constitutes a fraction of the exhaust N_{LE} coming from the top of the other column that is completely devoid of the heavy component (that is, $y_{A,L} = 0.0$). The feed location is chosen such that the composition of the feed $y_{A,F}$ matches that in the column. The exhaust gas leaving the column N_{HE} at P_L is completely devoid of light component (that is, $y_{A,H} = 1.0$). This gas is compressed to P_H, and a fraction is taken off as heavy product N_{HP} while the rest N_{HF} is recycled to the other column as heavy reflux. Step 1 (and, hence, step 3) ends just at the moment the light component reaches the bottom of the column, which ensures that the heavy product is always pure in the heavy component. Since step 1 is the low constant pressure step of the cycle, and since the compositions of the two feed streams N_F and N_{LF} are both necessarily less than $y_A = 1.0$, this step constitutes a desorption step. N_F and N_{LF} both collectively lower the concentration of the heavy component in the gas phase, which in turn causes the heavy component to desorb and be swept toward the enriching section of the column. Clearly, N_{LF} (and to some extent even N_F) serves the same role as low pressure purge does in a traditional SR PSA process.

During Step 2, the countercurrent pressurization step, the column is completely pressurized from P_L to P_H with gas N_{Bl} from the other column undergoing step 4 (depressurization). This step is accomplished by connecting the bottoms of the two columns together through a pump, with the tops of the two columns closed. There are two unique features of this pressurization step: First $N_{Pr} = N_{Bl}$, and second, the composition of the pressurization gas N_{Pr} (and, hence, N_{Bl}) is always pure in the heavy component (that is, $y_{A,H} = 1.0$). The first feature is a consequence of the linear isotherm assumption (Ebner and Ritter, 2002), whereas the second feature is a design constraint that stipulates the heavy product N_{HP} must always be pure in the heavy component.

During step 3, the high-pressure column is essentially being fed countercurrently with heavy reflux N_{HF}, which is necessarily pure in the heavy component. The exhaust gas N_{LE} leaving the column during this step is necessarily pure in the light component. A small fraction of this gas is expanded from P_H to P_L through a valve or orifice and recycled to the other column as light reflux N_{LF}. The rest of it is taken off at P_H as the light product N_{LP}. Step 3 (and, hence, step 1) ends just at the moment the heavy component reaches the top of the the column, which ensures that the light product is always pure in the

light component. Since step 3 is the high-pressure step of the cycle, and since the heavy reflux stream N_{HF} necessarily contains the highest concentration of the heavy component, this step constitutes an adsorption step. N_{HF} increases the concentration of the heavy component in the gas phase, which in turn causes the heavy component to adsorb, leaving less of the heavy component to be swept toward the stripping section of the column. Clearly, N_{HF} serves the same role as high pressure feed does in a traditional SR PSA process.

During step 4, the cocurrent depressurization or blowdown step, the column is completely depressurized from P_H to P_L by removing N_{Bl} from the bottom of the column. As noted earlier, this gas is used to completely pressurize the other column undergoing step 2 by directing it through the pump, with the tops of the two columns closed. Also, $N_{Bl} = N_{Pr}$, and the composition of the blowdown gas N_{Bl} (and, hence, N_{Pr}) is always pure in the heavy component (that is, $y_{A,H} = 1.0$). Although seemingly obscure, these uniquely coupled pressure varying steps can be viewed as two pressure varying steps occurring in series: The first step is an equalization step, where the two columns connected through the bottoms of the columns equalize to pressure P_{eq} (that is, $P_H \rightarrow P_{eq}$ and $P_L \rightarrow P_{eq}$). The second step is a heavy product pressurization step also carried out through the bottoms of the columns, where $P_{eq} \rightarrow P_L$ in one column, and $P_{eq} \rightarrow P_H$ in the other column.

Equalization is commonly used in conventional SR PSA processes to save compression energy. In contrast, heavy product pressurization is not generally practiced. Instead, feed or light product pressurization is commonly used, because the goal is typically to produce a very pure light product via a SR PSA cycle. In retrospect, the use of a heavy product pressurization step makes sense when the goal is to produce a very pure heavy product (Ebner and Ritter, 2002). However, when the goal is to produce two very pure products from a binary feed, for example, with the DR PSA cycle just described, the selection of the pressurization/blowdown mode becomes a challenging design issue. The mode chosen in this study, mostly to make the analysis tractable, represents only one, yet interesting, pressurization/blowdown mode for a DR PSA cycle. Many other variants are possible, as can be envisioned from the above discussion.

Mathematical Model

The partial and total mole balance equations describing the adsorption dynamics of heavy component A in an ideal binary gas mixture within an isothermal bed, where irreversible phenomena, such as diffusion, dispersion and other mass-transfer mechanisms are neglected, are respectively given by

$$\varepsilon\left(\frac{\partial P_A}{\partial t} + \frac{\partial u P_A}{\partial z}\right) + RT(1-\varepsilon)\frac{\partial n_A}{\partial t} = 0 \tag{1}$$

$$\varepsilon\left(\frac{\partial P}{\partial t} + \frac{\partial u P}{\partial z}\right) + RT(1-\varepsilon)\frac{\partial n}{\partial t} = 0 \tag{2}$$

with

$$P = P_A + P_B, \quad n = n_A + n_B \tag{3}$$

u is the interstitial velocity, P is the absolute pressure, P_i is the partial pressure of species i (either A or B), ε is the bed void fraction, n_i is the moles of species i per unit volume of bed, T is the absolute temperature, and R is the universal gas constant. For simplicity and as a first approximation, the isotherms are assumed to be linear and given by

$$n_i = \frac{k_i P_i}{RT} = \frac{k_i P y_i}{RT} \quad i = A \text{ or } B \tag{4}$$

where k_i is the dimensionless Henry's law constant of species i, and y_i is the gas-phase mole fraction of species i.

According to equilibrium theory and defining (Knaebel and Hill, 1985)

$$\beta_i = \frac{1}{1 + (1-\varepsilon)k_i/\varepsilon}, \quad i = A \text{ or } B \tag{5}$$

it can be shown that, within a column where the pressure drop along the bed is assumed to be negligible, the interstitial velocity u at a given location z, where the concentration is y_A, is given by

$$u = \frac{-z}{\beta_B(1 + (\beta - 1)y_A)}\frac{1}{P}\frac{\partial P}{\partial t} \tag{6}$$

for the pressurization and blowdown steps with the bed closed at one end (that is, $u = 0$) at $z = 0$ (here, the light product end).

For the constant pressure steps, the relationship between the interstitial velocities at any two locations m and n in the bed, is given by

$$\frac{u_m}{u_n} = \frac{(1 + (\beta - 1)y_{A,n})}{(1 + (\beta - 1)y_{A,m})} \tag{7}$$

where the parameter β is defined as

$$\beta = \frac{\beta_A}{\beta_B} \tag{8}$$

and represents the selectivity of the adsorbent toward the two species. Because a smaller value of β_i corresponds to a larger affinity of the adsorbent for component i, β varies between 0 and 1.

For concentration profiles that are entirely characterized by simple waves, the characteristics for the constant pressure steps are given by

$$y_A = y_{A,o} \tag{9a}$$

$$z = z_o + \frac{\beta_A u \Delta t}{1 + (\beta - 1)y_A} \tag{9b}$$

where Δt is the duration of the constant pressure step. For the pressure varying steps, the characteristics are given by

$$\frac{y_A}{y_{A,o}} = \left(\frac{1 - y_A}{1 - y_{A,o}}\right)^{\beta} \pi^{(\beta-1)}, \quad \pi = P/P_o \tag{10a}$$

$$\frac{z}{z_o} = \left(\frac{y_{A,o}}{y_A}\right)^{(\beta+1)/\beta} \left(\frac{1 + (\beta - 1)y_A}{1 + (\beta - 1)y_{A,o}}\right) \pi^{-1/\beta} \tag{10b}$$

where the subscript o stands for the initial temporal condition of the characteristic. The characteristics representing shock waves are not presented here, because they are not required in the ensuing analysis.

To determine the dependence of the performance parameters, such as the two recycle ratios and the throughput, on the pressure ratio, feed concentration, and selectivity, the dependence of N_{HF}, N_{HE}, N_{LF}, and N_{LE} on the total moles N_F entering the bed during the feed step must be determined. Recall that the DR PSA cycle described in the previous section completely separates the binary feed into two pure components; thus, the mole fractions of the heavy component A in all the heavy ($y_{A,H}$ in N_{HE}, N_{HF}, and N_{HP}) and light product flows ($y_{A,L}$ in N_{LF}, N_{LE}, and N_{LP}) are equal to 1 and 0, respectively. By defining the light product volumetric purge to feed ratio (that is, u_{LF}/u_F) as γ_L, and the heavy product volumetric purge to feed ratio (that is, u_{HF}/u_F) as γ_H

$$N_{LF} = \frac{P_L}{RT} u_{LF} \varepsilon A_{cs} \Delta t = \gamma_L N_F = \gamma_L \phi \Delta \tau \tag{11}$$

and

$$N_{HF} = \frac{P_H}{RT} u_{HF} \varepsilon A_{cs} \Delta t = \pi_T \gamma_H N_F \tag{12}$$

where N_F is the total number of moles fed to the column during time Δt, that is

$$N_F = \frac{P_L}{RT} u_F \varepsilon A_{cs} \Delta t \tag{13}$$

$\pi_T = P_H/P_L$, and ϕ and $\Delta\tau$ are given by

$$\phi \equiv \frac{\varepsilon A_{cs} L}{RT} \left(\frac{P_L}{\beta_A}\right) \tag{14}$$

$$\Delta\tau \equiv \frac{u_F}{L} \beta_A \Delta t \tag{15}$$

and A_{cs} is the cross-sectional area of the column. u_F, the interstitial velocity associated with the feed, is defined in terms of A_{cs} for convenience.

Since the addition of the feedstream essentially produces a discontinuity in the flow profile in the bed at the feed location, the relationship between N_{HE} and N_F is obtained by defining the interstitial velocities in the bed just upstream and just downstream of the feed location as u_F^- and u_F^+, respectively. This relationship is shown in Figure 2. By realizing that

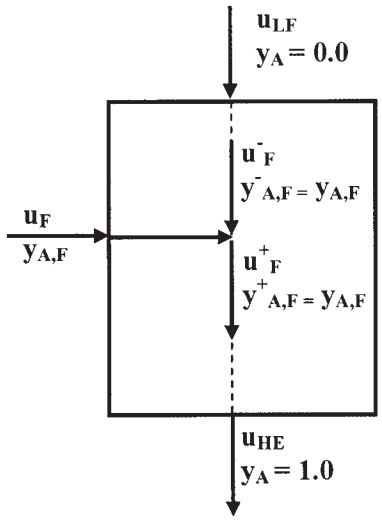

Figure 2. Discontinuity of the flow profile in the column at the feed location.

The velocities u_F^+ and u_F^- are the interstitial velocities just upstream, and just downstream of the feed location, respectively. The concentration of the heavy component is always assumed to be equal to $y_{A,F}$ at the feed location.

$$u_F^+ = u_F + u_F^- \tag{16}$$

and by forcing the concentration in the column at the feed location to be equal to y_F (that is, no blending,) at all times during the feed step, it is easy to show from Eqs. 7 and 16 that

$$u_F^- = \frac{u_{LF}}{(1 + (\beta - 1)y_{A,F})} = \gamma_L \frac{u_F}{(1 + (\beta - 1)y_{A,F})} \tag{17}$$

$$u_F^+ = u_F + u_F^- = \left(1 + \frac{\gamma_L}{(1 + (\beta - 1)y_{A,F})}\right) u_F \tag{18}$$

$$u_{HE} = \frac{(1 + (\beta - 1)y_{A,F})}{\beta} u_F^+ = \frac{(1 + (\beta - 1)y_{A,F} + \gamma_L)}{\beta} u_F \tag{19}$$

During the feed step, the column is modeled as two columns in series. The first column has length z_F with inlet conditions $u = \gamma_L u_F$ and $y_A = 0$, and outlet conditions $u = u_F^- = \gamma_L u_F/(1+(\beta-1)y_{A,F})$ and $y_A = y_{A,F}$. The second column has length $L - z_F$ with inlet conditions $u = u_F^+ = u_F\,(1 + \gamma_L/(1+(\beta-1)y_{A,F}))$ and $y_A = y_{A,F}$, and outlet conditions $u = u_{HE}$ and $y_A = 1$. Hence

$$N_{HE} = \frac{(1 + (\beta - 1)y_{A,F} + \gamma_L)}{\beta} N_F \tag{20}$$

and

$$N_{LE} = \frac{P_H}{RT} u_{LE} \varepsilon A_{cs} \Delta t = \pi_T \gamma_H \beta N_F \tag{21}$$

because $u_{LE} = \beta u_{HF}$ according to Eq. 7. It is noteworthy that the imposed condition $y^{+}_{A,F} = y^{-}_{A,F} = y_{A,F}$ not only avoids undesirable back mixing and dilution in the bed at the feed location, it also allows analytical expressions to be obtained for all the important performance indicators of a DR PSA cycle, as shown later.

In the case of N_{Pr} and N_{Bl}, because the gas at the bottom of each of the columns is pure in the heavy component A, according to Eq. 6, the interstitial velocities at these locations are given by the following identical expressions

$$u_{\mathrm{Pr}} = -\frac{L}{\beta_B \beta}\frac{1}{P}\frac{\partial P}{\partial t} = -\frac{L}{\beta_A}\frac{1}{P}\frac{\partial P}{\partial t} \tag{22a}$$

$$u_{Bl} = -\frac{L}{\beta_A}\frac{1}{P}\frac{\partial P}{\partial t} \tag{22b}$$

However, the pressure and its time derivative at any given time may be different in each column; thus, u_{Pr} and u_{Bl} are not necessarily identical. According to Eq. 22a, it is straightforward to integrate the total flow entering the column undergoing pressurization to obtain N_{Pr} as

$$N_{\mathrm{Pr}} = \int_0^{\Delta t_{PV}} \frac{P}{RT} u_{\mathrm{Pr}} \varepsilon A_{cs} dt = \int_{P_L}^{P_H} \frac{1}{RT}\frac{L}{\beta_A} \varepsilon A_{cs} dP = \phi(\tau_T - 1) \tag{23}$$

Similarly, according to Eq. 22b, N_{Bl} is given by

$$N_{Bl} = \phi(\pi_T - 1) \tag{24}$$

which is identical to N_{Pr}. This important result is simply a consequence of fact that the isotherms used here are linear. In general, N_{Pr} and N_{Bl} are not equal in systems with nonlinear isotherms, where typically $N_{Bl} < N_{Pr}$. In such a case, an extra term either in the form of a product stream or a recycle stream is needed to make up the difference between N_{Pr} and N_{Bl}.

At the periodic state, each bed necessarily returns to its original state after the completion of every cycle; hence, the following relationship must be maintained

$$N_F + N_{LF} - N_{HE} + N_{HF} - N_{LE} + N_{\mathrm{Pr}} - N_{Bl} = 0 \tag{25}$$

Now, combining Eqs. 11 through Eqs. 15, 20, 21, 23, and 24 gives the heavy product molar purge to feed ratio ($\gamma_H \pi_T$) as

$$\gamma_H \tau_T \equiv \frac{N_{HF}}{N_F} = \left(\frac{1 - y_{A,F} + \gamma_L}{\beta}\right) \tag{26}$$

The corresponding recycle ratios of the light and heavy products are, respectively, given by

$$R_L \equiv \frac{N_{LF}}{N_{LE}} = \left(\frac{\gamma_L}{1 - y_{A,F} + \gamma_L}\right) = \left(\frac{\beta \gamma_H \tau_T + y_{A,F} - 1}{\beta \gamma_H \pi_T}\right) \tag{27}$$

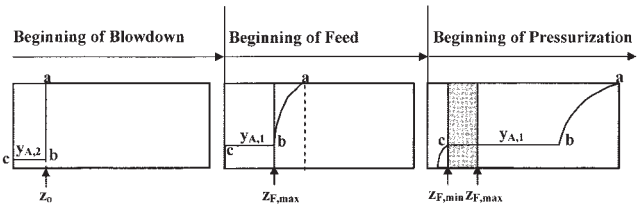

Figure 3. Pictorial description of the locations of $z_{F,\min}$ and $z_{F,\max}$ in a DR-PSA column.

Each plot represents the initial concentration profiles of the heavy component in the column at the (a) beginning of blowdown, (b) beginning of feed, and (c) end of feed. Tags a, b and c represent the locations of three different characteristics that are associated with the concentration front of the heavy component as it moves through the column during each step. The blowdown step is assumed to start from a fully developed shock wave, as indicated in (a). Locations $z_{F,\min}$ and $z_{F,\max}$ are determined from the positions of the characteristics c and b at the end and beginning of the feed step, respectively.

$$R_H \equiv \frac{N_{HF}}{N_{HE}} = \left(\frac{1 - y_{A,F} + \gamma_L}{1 + (\beta - 1) y_{A,F} + \gamma_L}\right) = \left(\frac{\gamma_H \pi_T}{y_{A,F} + \gamma_H \pi_T}\right) \tag{28}$$

These two recycle ratios represent the fraction of gas leaving one column that is returned to the other column. They are more convenient to use here than the related reflux ratios (Diagne et al. 1994, 1995, 1996) because their values range between 0 and 1.

Figure 1 shows that two broad plateaus of constant concentration exist in the middle and upper sections of the columns. During the constant pressure steps, these two plateaus, denoted by $y_{A,1}$ and $y_{A,2}$, correspond to concentrations (characteristics) that persist during the feed and purge steps, respectively. They are related to each other through Eq. 10 according to

$$\frac{y_{A,2}}{y_{A,1}} = \left(\frac{1 - y_{A,2}}{1 - y_{A,1}}\right)^{\beta} \pi_T^{(\beta - 1)} \tag{29}$$

Because it has been assumed that the concentration at the feed location is equal to $y_{A,F}$ at all times during the feed step, the value of $y_{A,1}$ in Eq. 29 is equal to $y_{A,F}$. While following the displacement of these plateaus within the column over time, it is readily reckoned that the feed location is not necessarily restricted to a fixed position. If the concentration in the column at the feed location is to be maintained at $y_{A,F}$, then the feed location can be placed anywhere between two locations, for example, $z_{F,\min}$ and $z_{F,\max}$, which in Figure 1 are depicted by the dashed lines cutting across the columns on either side of the arrow representing the feed. Figure 3, which shows very clearly what happens to the concentration profile in one column during blowdown, feed and pressurization, is used to explain this rather unique situation.

From left to right, Figure 3 shows the initial concentration profiles of the heavy component in the column for the blowdown, feed, and pressurization steps. It is assumed that at the beginning of the blowdown step the concentration profile of the heavy component is characterized by a fully developed shock wave that forms at the end of the previous purge step (step 3), as alluded to in Figure 1. During blowdown, the shock wave

immediately transforms into a simple wave, the trailing edge of which must be located just downstream of the feed location z_F by the end of this step; this edge defines the location of $z_{F,\max}$ as shown. During feed, a second simple wave develops at $z = 0$ due to N_{LF} having a y_A necessarily less than $y_{A,1}$. The leading edge of this simple wave must be located just upstream of the feed location z_F by the end of this step; this edge defines the location of $z_{F,\min}$ as shown. The location $z_{F,\min}$ ($< z_F$) ensures that the feed concentration never blends with the lower upstream concentration front at the end of the feed step, whereas the location $z_{F,\max}$ ($> z_F$) ensures that the feed concentration never blends with the higher downstream concentration front at the beginning of the feed step.

It is easy to observe in Figure 3 that $z_{F,\min}$ actually corresponds to the location of characteristic c at the end of feed (or beginning of pressurization). From Eqs. 7, Eq. 9b (for which $z_o = 0$, $u = u_m$, $u_n = u_{LF}$, $y_A = y_{A,m} = y_{A,F}$ and $y_{A,n} = 0$ in Eqs. 7 and 9b), and the definition of $\Delta\tau$ in Eq. 15, $z_{F,\min}$, is given by

$$\frac{z_{F,\min}}{L} = \frac{\gamma_L \Delta\tau}{(1 + (\beta - 1)y_{A,F})^2} \tag{30}$$

Similarly, $z_{F,\max}$ corresponds to the location of characteristic b at the beginning of feed (or end of blowdown). Since characteristic b shares the same location z_o as characteristic a at the beginning of blowdown (because both are members of the same shock wave), from Eq. 10b and $\pi = 1/\pi_T$

$$\frac{z_a}{z_o} = \left(\frac{y_{A,o}}{y_{A,2}}\right)^{(\beta+1)/\beta}\left(\frac{1 + (\beta - 1)\,y_{A,2}}{1 + (\beta - 1)\,y_{A,o}}\right)\pi_T^{1/\beta} \tag{31.a}$$

$$\frac{z_b}{z_o} = \frac{z_{\max}}{z_o} = \left(\frac{y_{A,o}}{y_{A,F}}\right)^{(\beta+1)/\beta}\left(\frac{1 + (\beta - 1)y_{A,F}}{1 + (\beta - 1)y_{A,o}}\right)\pi_T^{1/\beta} \tag{31.b}$$

Eliminating z_o from these equations gives the following relationship that relates $z_{F,\max}$ with the location of characteristic a at the end of blowdown

$$\frac{z_b}{z_a} = \frac{z_{F,\max}}{z_a} = \left(\frac{y_{A,2}}{y_{A,F}}\right)^{(\beta+1)/\beta}\left(\frac{1 + (\beta - 1)y_{A,F}}{1 + (\beta - 1)y_{A,2}}\right) \tag{32}$$

Note the absence of a pressure term in Eq. 32, which is due to the fact that z_b and z_a share the same location z_o at the beginning of blowdown. It is even more important to realize that z_b and z_a correspond to the locations of two altogether different characteristics at the same instant in time and pressure (that is, beginning of the feed step) and not to two different locations of the same characteristic at different moments of a pressure changing process, as with z and z_o in Eq. 10b.

Since Δt is the duration of the feed step, it is also the time that it takes characteristic a to reach the bottom of the column (that is, $z = L$). At the beginning of the fed step, z_A can also be defined by a constant α that arbitrarily denotes the relative location of z_A with respect to the end of the column, that is

$$\alpha \equiv \frac{L - z_a}{L} \tag{33}$$

This allows z_a in Eq. 32 to be eliminated, which leads to

$$\frac{z_{F,\max}}{L} = \left(\frac{y_{A,2}}{y_{A,F}}\right)^{(\beta+1)/\beta}\left(\frac{1 + (\beta - 1)y_{A,F}}{1 + (\beta - 1)y_{A,2}}\right)(1 - \alpha) \tag{34}$$

The mole fraction $y_{A,2}$ (see Figure 3) is related to the feed concentration $y_{A,F}$ through Eq. 29 (where $y_{A,1} = y_{A,F}$). It is also easy to show from Eqs. 7 and 9b, and the definitions of $\Delta\tau$ and u_{HE} in Eqs. 15 and 19, that for characteristic a (for which $z_o = z_a$, $z = \mathrm{L}$, $u_{\mathrm{m}} = u$, $u_{\mathrm{n}} = u_{\mathrm{HE}}$ and $y_A = y_{\mathrm{A,m}} = y_{\mathrm{A,n}} = 1$ in Eqs. 7 and 9b), α is also equal to

$$\alpha \equiv \frac{\Delta\tau}{\Delta\tau_{\max}} \tag{35}$$

with $\Delta\tau_{\max}$ given by

$$\Delta\tau_{\max} = \frac{\beta^2}{1 + (\beta - 1)y_{A,F} + \gamma_L} \tag{36a}$$

From Eq. 26, $\Delta\tau_{\max}$ can also be expressed in terms of the heavy product molar purge to feed ratio as

$$\Delta\tau_{\max} = \frac{\beta}{y_{A,F} + \gamma_H \pi_T} \tag{36b}$$

$\Delta\tau_{\max}$ is the dimensionless time it takes characteristic a to travel from the top of the column ($z = 0$) to the bottom of the column ($z = L$) during the constant pressure feed step. Since, in principle, this characteristic can start from anywhere in the column, $\Delta\tau_{\max}$ corresponds to the maximum duration of the constant pressure step, which naturally leads to $\alpha = 1$ in this case.

The throughput θ, defined in the usual way as the amount of feed processed per unit time per unit mass of bed, is given by Eq. 37 in terms of the volumetric flow rate at STP

$$\theta = \left[\frac{1}{2}\frac{P_L T_{STP}}{P_{STP} T}\frac{\varepsilon}{\rho_s(1 - \varepsilon)}\frac{u_F}{L}\right]\frac{\Delta t}{\Delta t + \Delta t_{PV}} \tag{37}$$

By defining χ as the ratio between the duration of the pressure varying (Δt_{PV}) and constant pressure (Δt) steps, that is

$$\chi = \frac{\Delta t_{PV}}{\Delta t} \tag{38}$$

and using Eqs. 15 and 35, the throughput can also be expressed as

$$\theta = \left[\frac{1}{2}\frac{P_L T_{STP}}{P_{STP} T}\frac{\varepsilon}{\rho_s(1 - \varepsilon)}\frac{1}{\Delta t \beta_A}\right]\frac{\alpha\Delta\tau_{\max}}{(1 + \chi)} \tag{39}$$

By defining the term in brackets as a characteristic throughput θ^*, Eq. 39 can be made dimensionless as

$$\Theta = \frac{\theta}{\theta^*} = \frac{\alpha \Delta \tau_{\max}}{(1+\chi)} \tag{40}$$

To determine the value of χ, it is assumed that the pump maintains the same velocity u_{pump} regardless of the pressure in each column, and, thus, regardless of the cycle step. Now, since the pump is located at the bottom of each of the columns, during the feed step it is further assumed that u_{pump} is identical to u_{HE}; thus

$$u_{\mathrm{pump}} = u_{HE} = \frac{(1 + (\beta - 1)y_F + \gamma_L)}{\beta} u_F \tag{41}$$

Because u_{pump} is constant and equal to u_{HE}, Eq. 41 can be substituted into in Eq. 6; the resulting equation can be integrated from $t = 0$ to $t = \Delta t_{PV}$. Equation 36b is then combined with the integrated expression, which when rearranged leads to

$$\chi = \frac{\beta \ln \pi_T}{\alpha \Delta \tau_{\max}(1 + (\beta - 1)y_F + \gamma_L)} = \frac{\ln \pi_T}{\alpha \beta} \tag{42}$$

Equation 42 is a very simple relationship that depends solely on the pressure ratio π_{T}, the selectivity β and the arbitrary constant α defined in Eq. 33 or 35. Substituting Eqs. 36a and 34 into Eq. 38 gives the dimensionless throughput Θ as

$$\Theta = \frac{\theta}{\theta^*} = \frac{1}{[1 + \ln \pi_T/(\alpha\beta)]} \frac{\alpha\beta^2}{[1 + (\beta - 1)y_{A,F} + \gamma_L]} \tag{43}$$

Results and Discussion

The dependence of the recycle ratios R_L and R_H, heavy product molar purge to feed ratio $\gamma_H \pi_T$, and dimensionless time $\Delta \tau_{\max}$ on the selectivity β, feed concentration $y_{A,F}$ and light product volumetric purge to feed ratio γ_L are shown in Figure 4. The results were obtained directly from Eqs. 26, 27, 28, and 36a. The graphs on the left (a1, b1, c1, and d1) were generated with $\gamma_L = 0.1$; and the graphs on the right (a2, b2, c2, and d2) were generated with $y_{A,F} = 0.2$. One of the most important objectives of this analysis is to show that the DR PSA cycle, when restricted to the condition of complete separation of a binary feed, is absolutely feasible. This means the conditions must be such that two pure products can always be produced; in other words, $\mathrm{R_L} \leq 1.0$ and $\mathrm{R_H} \leq 1.0$. Figures 4a1, 4a2, 4b1 and 4b2 show that, under the theoretical framework considered in this study, these constraints are met over a wide range of conditions. $\mathrm{R_L}$ is also essentially independent of β and only influenced by $y_{A,F}$ and γ_L. Although Eq. 27 confirms this independence (which means that $\mathrm{R_L}$ does not depend on the identity of the components of the gases being separated), this result is simply an artifact of choosing γ_L as the independent variable. With $\gamma_H \pi_T$ chosen as the independent variable, R_L does indeed depend on β. In fact, R_L indirectly depends on β through the dependence of γ_L on $\gamma_H \pi_T$, as governed by Eq. 26.

In contrast, $\mathrm{R_H}$ readily approaches unity for small $y_{A,F}$ and β, and large γ_L. However, this does not imply that the cycle under these most extreme conditions is becoming infeasible. This result is simply a consequence of the fact that as β or $y_{A,F}$ decrease, or γ_L increases, the amount of heavy component that

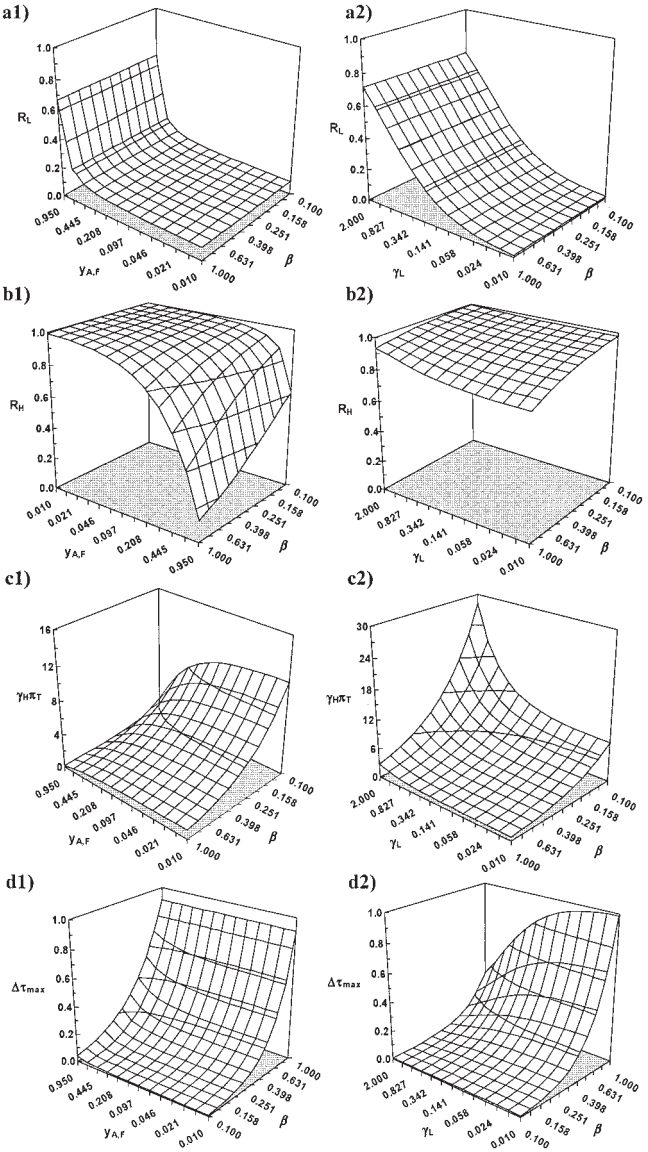

Figure 4. Effect of the selectivity β, feed concentration $y_{A,F}$, and light product purge to feed ratio γ_L on the (a) light product recycle R_L, (b) heavy product recycle R_H, (c) heavy product molar purge to feed ratio $\gamma_H \pi_T$, and (d) $\Delta \tau_{max}$ as defined in Eq. 33.

Graphs on the left show the effect of β and $y_{A,F}$ with $\gamma_L = 0.1$; graphs on the right show the effect of β and γ_L with $y_{A,F} = 0.2$.

desorbs during the low-pressure feed step also increases, which directly impacts N_{HE}. Since this DR PSA cycle always produces a pure heavy product, for high selectivities (smaller β) and low feed concentrations, virtually all N_{HE} must be recycled as N_{HF}, which necessarily causes R_H to be very close to, but still less than unity. In fact, for a fixed feed concentration, as in Figure 4b2, N_{HP} is also fixed; so, as β decreases or as γ_L increases, the resulting increase in the desorption of the heavy component causes N_{HE} to increase. However, since N_{HP} is fixed, N_{HF} (and, hence, R_H) must increase to compensate for the increase in N_{HE}. This also explains why the values of R_H are

always in the neighborhood of unity when the feed concentration is relatively low at $y_{A,F} = 0.2$, as shown in Figure 4b2, which appears somewhat misleadingly as a relatively weak dependence of R_H on γ_L or β. It is similarly argued that, when the feed concentration is very high (Figure 4b1), the strong dependence of R_H on β is caused by the increase in desorption that accompanies a decrease in β (higher selectivity). A similar explanation is offered for the dependence of the heavy product molar purge to feed ratio $\gamma_H\pi_T$ on $y_{A,F}$, β and γ_L.

Figures 4c1 and 4c2 show that $\gamma_H\pi_T$ is essentially independent of $y_{A,F}$, β and γ_L, except at low values of β. Clearly, only when the selectivity is very high (small β) does $\gamma_H\pi_T$ need to increase substantially to compensate for the increase in N_{HE} due to desorption. This is especially true when $y_{A,F}$ is low (Figure 4c1), or when γ_L is large even when $y_{A,F}$ is relatively low at 0.2 (Figure 4c2). The relatively weak dependence of $\gamma_H\pi_T$ on $y_{A,F}$, β and γ_L over such a wide range of conditions suggests that, for the case when the feed concentration is fixed (Figure 4c2), the internal flows that manifest through γ_L and $\gamma_H\pi_T$ need to adjust only slightly to account for changes in selectivity, until β becomes very small. Similarly, for the case when γ_L is fixed (Figure 4c1), the internal flows that manifest through $\gamma_H\pi_T$ and N_{HP} need to adjust only slightly to compensate for changes in both $y_{A,F}$ and β, until both these variables are very small. The effects of $y_{A,F}$, β and γ_L on $\Delta\tau_{max}$, shown in Figures 4d1 and 4d2, further elucidate the subtle features associated with the sometimes intense heavy component desorption flows of a DR PSA cycle.

The dependence of $\Delta\tau_{max}$ on β seems counterintuitive, because as the selectivity increases (smaller β), $\Delta\tau_{max}$ decreases. Recall, however, that $\Delta\tau_{max}$ is the time it takes the characteristic corresponding to the pure heavy component concentration to traverse the entire length of the column during the low-pressure feed (or desorption) step. Hence, this counterintuitive result is again due to the increase in the heavy component desorption flow that ensues with decreasing β; and the effect obviously becomes more pronounced as γ_L increases. The greater this desorption flow, the greater the increases in the interstitial velocities along the column toward the heavy product end, and the shorter the time it takes characteristic a to traverse the column; hence, $\Delta\tau_{\max}$ must decrease with decreasing β and increasing γ_L. Another counterintuitive result is the fact that with γ_L fixed and equal to 0.1, Figure 4d1 projects $\Delta\tau_{\max}$ to be essentially independent of the feed concentration, despite the obvious dependence shown in Eq. 36a or 36b, that is, $\Delta\tau_{\max}$ should decrease with an increase in $y_{A,F}$. Apparently, the effect of the feed concentration is overwhelmed by the effect of the internal flows associated with the two volumetric purge to feed ratios γ_L and γ_H, which are coupled through Eq. 19. Eq. 36b expounds on this explanation in that the value of $y_{A,F}$, varying only between 0 and 1, is effectively dwarfed by the effect of β.

It is worth making one last comment about the graphs in Figure 4. Notice that Eqs. 26, 27, 28 and 36a do not contain the pressure ratio π_T as an independent variable. Thus, it appears that the recycle ratios R_L and R_H, heavy product molar purge to feed ratio $\gamma_H\pi_T$, and dimensionless time $\Delta\tau_{\max}$, when plotted in terms of β, $y_{A,F}$ and γ_L, are all independent of π_T. Again, this result is an artifact of choosing γ_L as the independent variable. In fact, Eqs. 26, 27, 28 and 36b show that with $\gamma_H\pi_T$ chosen as the independent variable, R_L, R_H, β and $\Delta\tau_{\max}$ do indeed depend on π_T. Nevertheless, it is quite interesting that the key parameters in a DR PSA cycle can be studied independently of π_T.

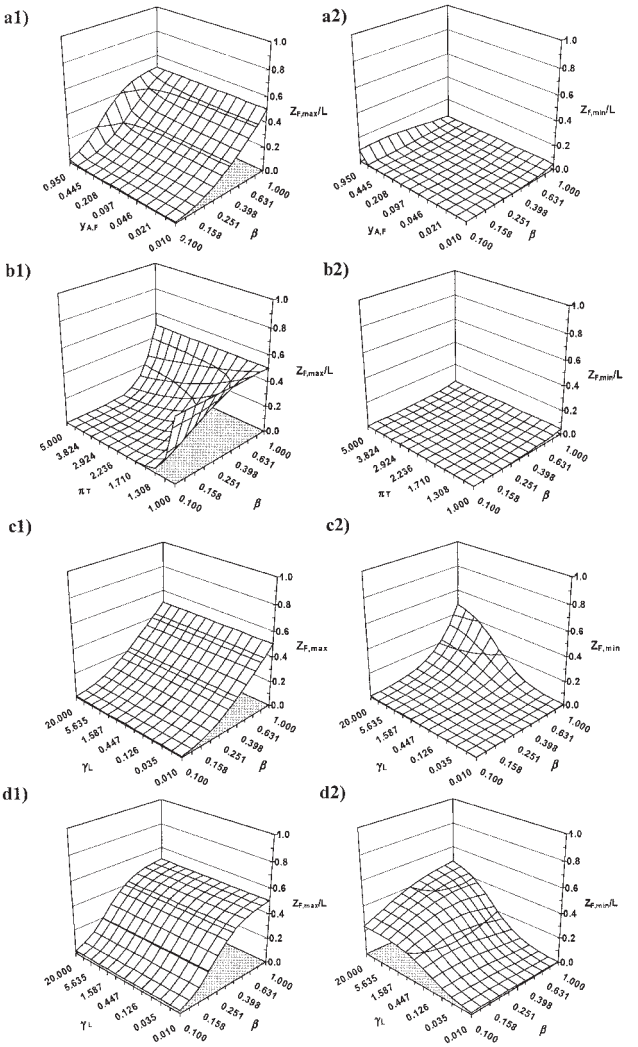

Figure 5. Effect of the selectivity β, feed concentration $y_{A,F}$, pressure ratio π_T, and light product purge to feed ratio γ_L on $z_{F,\max}$ (graphs on the left), and $z_{F,\min}$ (graphs on the right) with $\Delta\tau = 0.5\,\Delta\tau_{\max}$.

(a) The effect of $y_{A,F}$ and β with $\pi_T = 1.5$ and $\gamma_L = 0.1$, (b) the effect of π_T and β with $y_{a,F} = 0.2$ and $\gamma_L = 0.1$, and the effect of γ_L and β with $\pi_T = 1.5$, and (c) $y_{a,F} = 0.2$, and (d) $y_{a,F} = 0.95$.

The dependences of $z_{F,\min}$ and $z_{F,\max}$ on β, $y_{A,F}$, π_T and γ_L are shown in Figure 5. The results were obtained for an arbitrary value of α ($\Delta\tau/\Delta\tau_{\max}$) = 0.5. The graphs on the left (a1, b1, c1 and d1) correspond to $z_{F,\max}/L$; and the graphs on the right (a2, b2, c2 and d2) correspond to $z_{F,\min}/L$. Figure 5a shows the effect of $y_{A,F}$ and β with $\pi_T = 1.5$ and $\gamma_L = 0.1$; Figure 5b shows the effect of π_T and β with $y_{A,F} = 0.2$ and $\gamma_L = 0.1$; Figure 5c shows the effect of γ_L and β with $\pi_T = 1.5$ and $y_{A,F} = 0.2$; and Figure 5d shows the effect of γ_L and β with $\pi_T = 1.5$, and $y_{A,F} = 0.95$. The selectivity β, and then the pressure ratio π_T and feed concentration $y_{A,F}$ have the greatest impact on the location of $z_{F,\max}/L$. For the entire ranges of π_T

and $y_{A,F}$, as β decreases, $z_{F,\max}/L$ approaches zero, and this occurs much more rapidly as π_T increases and $y_{A,F}$ decreases, as shown in Figures 5b1 and 5a1, respectively. In contrast, Eq. 34 shows $z_{F,\max}/L$ to be completely independent of γ_L, which is verified in Figure 5d1. The effect of β, $y_{A,F}$ and γ_L on $z_{F,\min}/L$ is much different, however.

The light product volumetric purge to feed ratio γ_L has the greatest effect on $z_{F,\min}/L$, especially when coupled with the effect of β. However, with $\gamma_L = 0.1$ (Figures 5a2 and 5b2), there is essentially no dependence of $z_{F,\min}/L$ on β, $y_{A,F}$, or π_T. $z_{F,\min}/L$ is either equal to zero or hovers just above $z/L = 0$ over very wide ranges of these parameters. In contrast, with $\pi_T = 1.5$ and for two different feed concentrations, $y_{A,F} = 0.2$ and $y_{A,F} = 0.95$, the effects of γ_L and β on $z_{F,\min}/L$ can be pronounced. At the lower $y_{A,F}$ (Figure 5c2), $z_{F,\min}/L$ hovers just above $z/L = 0$ for all γ_L at low β and for all β at low γ_L. However, as both these parameters increase, their effects on $z_{F,\min}/L$ increase substantially approaching $z/L = 0.5$ at the extremes. At the higher $y_{A,F}$ (Figure 5d2), the effects of γ_L and β are quite marked over the entire range of these variables, except at the lowest value of γ_L where, for any β, $z_{F,\min}/L$ is essentially equal to zero. In fact, over broad ranges of these parameters, $z_{F,\min}/L$ is located quite far away from $z/L = 0$, but again approaching $z/L = 0.5$ at the extremes.

Recall that the feed position z_F/L can be located anywhere between $z_{F,\min}/L$ and $z_{F,\max}/L$; in other words, $z_{F,\min}/L \leq z_F/L \leq z_{F,\max}/L$. The graphs in Figure 5 collectively reveal that, under certain conditions, z_F/L must be located very near $z/L = 0$, that is, only the enriching section of the column is needed to carry out the separation. In general, this tends to be true for low values of β (high selectivities) and γ_L, and somewhat true for high values of π_T, and low values of $y_{A,F}$. However, under a different set of conditions, z_F/L must be located very near $z/L = 0.5$, that is, both the stripping and enriching sections of the column are needed to carry out the separation. Not surprisingly, this tends to be true at the opposite conditions of where only a rectifier is needed. Over the intermediate ranges of these parameters, there is a wide range of conditions for which $z_{F,\max}$ is larger than $z_{F,\min}$. So, z_F/L can be located at or anywhere between these limits.

Another interesting aspect associated with the results shown in Figure 5, is the observation that under all the conditions investigated, the maximum limit for both $z_{F,\min}/L$ or $z_{F,\max}/L$ appears to be 0.5, which happens to be the arbitrarily chosen value of α. Indeed, when $\beta = 1$ (no selectivity), $y_{A,F}$ and $y_{A,2}$ become identical (Eq. 29) and, thus, Eq. 34 leads to

$$\frac{z_{F,\max}}{L} < \lim_{\beta \to 1} \frac{z_{F,\max}}{L} = 1 - \alpha \tag{44}$$

while if in addition to $\beta = 1$, the DR PSA unit operates under total recycle (that is, γ_L and, thus, $\gamma_H \to \infty$) Eqs. 30 and 36 lead to

$$\frac{z_{F,\min}}{L} < \lim_{\beta \to 1, \gamma_L \to \infty} \frac{z_{F,\min}}{L} = \alpha \tag{45}$$

Hence, the upper limits for $z_{F,\max}$ and $z_{F,\min}$ are $1-\alpha$ and α, respectively.

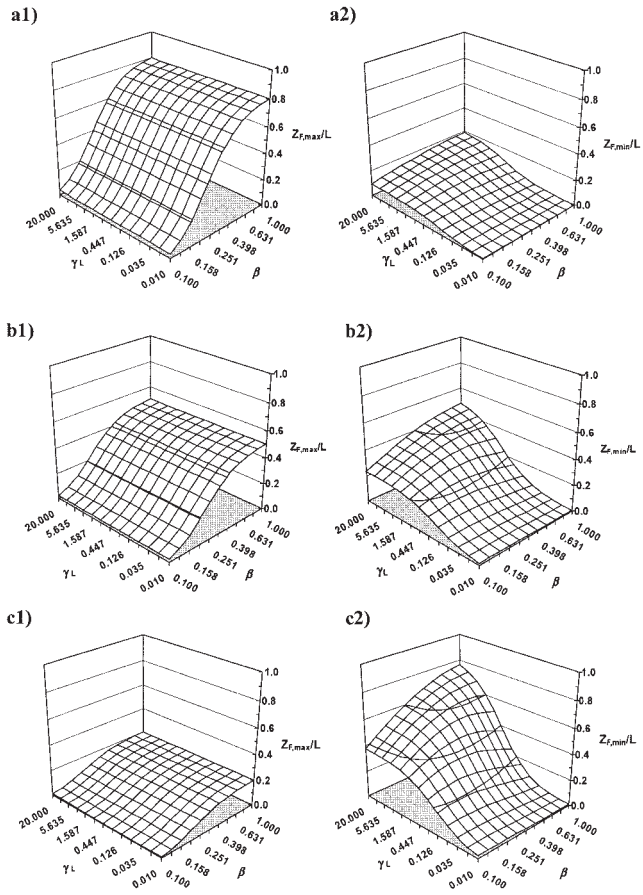

Figure 6. Effect of γ_L and β on $z_{F,\max}$ (graphs on the left) and $z_{F,\min}$ (graphs on the right), with $\pi_T = 1.5$, $y_{a,F} = 0.95$, and (a) $\alpha = 0.2$, (b) $\alpha = 0.5$, and (c) $\alpha = 0.8$.

To investigate the effect of α and its associated limits, three values of α are investigated in Figure 6 under identical conditions to those used in Figure 5d. Again, the graphs on the left (a1, b1 and c1) correspond to $z_{F,\max}/L$; and the graphs on the right (a2, b2 and c2) correspond to $z_{F,\min}/L$. All the figures show the effects of γ_L and β with $\pi_T = 1.5$ and $y_{A,F} = 0.95$; and $\alpha = 0.2$, 0.5, and 0.8 in Figures 6a, 6b, and 6c, respectively. Figures 6a1 and 6a2 show that when α is small ($\alpha = 0.2$), $z_{F,\max}/L$ and $z_{F,\min}/L$, respectively, approach limits of 0.8 and 0.2, in agreement with Eqs. 44 and 45. Moreover, when α is small, except for very low values of β (high selectivities), the feed can be located almost anywhere in the column up to $z/L = 0.8$ for the chosen set of conditions. As α increases, however, the range of z/L, where the feed can be located begins to decrease dramatically to the point where $z_{F,\min}/L$ becomes greater than $z_{F,\max}/L$. For example, when $\alpha = 0.8$, as in Figures 6c1 and 6c2, $z_{F,\min}/L > z_{F,\max}/L$ over a broad range of conditions, which severely limits the feed location to positions where back mixing does not occur (that is, $z_{F,\min}/L \leq z_{F,\max}/L$). It is noteworthy that no conclusions can be drawn under conditions where back mixing occurs, that is, $z_{F,\min}/L > z_{F\max}/L$, because the overly simplified model developed here is no longer valid in this situation. According to the definition of $\Delta\tau$ in Eq. 15 and also Eq. 35, excessively short columns (small L), large feed

velocities u_F, or long feed steps Δt may lead to conditions where the model is invalid.

The results in Figures 5 and 6 also allude to the fact that while there are many different conditions for which only an enriching section is needed to carry out the separation (for example, see Figure 5b1 for small β and large π_T, where both $z_{F,\max}$ and $z_{F,\min}$ are small and very close to zero), there is absolutely no complementary situation where only a stripping section is needed. In other words, conditions cannot be found such that $z_{F,\max}$ and $z_{F,\min}$ are both large and essentially equal to the bed length, mainly because of the constraints imposed on them through the value of α (Eqs. 44 and 45). Not surprisingly, this means that, under any circumstances, a long stripping section, when combined with a relatively short enriching section, cannot adequately handle the sometimes intense heavy component desorption flows associated with a DR PSA cycle, and still carry out the complete separation of a binary feed. In fact, from a feed location point of view, the results in Figures 5 and 6 tend to suggest that a small value of α is better, because it lessens the chance of backmixing. However, from a performance point of view, in terms of throughput, it turns out that a large value of α is indeed better, as can be gleaned from Eqs. 35 and 43. Hence, a compromise exists between minimizing the effects of back mixing and maximizing the throughput.

Figure 7 shows the dependence of the dimensionless throughput Θ (a1, b1, c1, and d1), and the corresponding heavy product molar purge to feed ratio $\gamma_H\pi_T$ (a2, b2, c2, and d2) on the pressure ratio π_T, feed concentration $y_{A,F}$, light product volumetric purge to feed ratio γ_L, α and selectivity β. The results for Θ were obtained from Eq. 43 and those for $\gamma_H\pi_T$ from Eq. 26. The value of the heavy product molar purge to feed ratio $\gamma_H\pi_T$ associated with each value of the dimensionless throughput Θ is included in Figure 7 to reveal the range and magnitude of the heavy component flow relative to Θ, because $\gamma_H\pi_T$ or equivalently R_H dictates the size of the pump that is needed by all DR PSA cycles to recycle part of the heavy exhaust N_{HE}. Figures 7a1 and 7a2 show the effects of π_T and β with $y_{A,F} = 0.1$, $\gamma_L = 0.2$ and $\alpha = 0.6$; Figures 7b1 and 7b2 show the effects of $y_{A,F}$ and β with $\pi_T = 2.0$, $\gamma_L = 0.2$ and $\alpha = 0.6$; Figures 7c1 and 7c2 show the effects of γ_L and β with $\pi_T = 2.0$, $y_{A,F} = 0.1$ and $\alpha = 0.6$; and Figures 7d1 and 7d2 show the effects of α and β with $\pi_T = 2.0$, $y_{A,F} = 0.1$ and $\gamma_L = 0.2$.

Figure 7a1 shows very clearly that, as π_T decreases and β increases (lower selectivity), Θ essentially goes from a value of zero up to a value as high as 0.5 when $\pi_T = \beta = 1.0$. Under these circumstances, Figure 7a2 shows that $\gamma_H\pi_T$ varies from 1 to 11 as β decreases from 1.0 to 0.1, but it is independent of π_T, as it should be. Nevertheless, the values of γ_H can be markedly higher than γ_L, and typically are much greater than γ_L at moderate pressure ratios and reasonable selectivities. A very similar trend is observed for Θ when γ_L and β both decrease, as shown in Figure 7c1. Figure 7c2 shows that $\gamma_H\pi_T$ also increases with increasing γ_L and decreasing β, approaching values of 30 at the extremes of these parameters. Again, γ_H tends to be many times that of γ_L, which is typical and quite understandable, especially when the feed concentration is relatively low (that is, $y_{A,F} = 0.1$). In contrast, Figure 7b1 shows that $y_{A,F}$ has essentially no effect on Θ; but that decreasing values of β again cause substantial decreases in the dimensionless throughput Θ, similarly to that shown in Figures 7a1 and 7c1. The effects of $y_{A,F}$ and β on $\gamma_H\pi_T$, shown in Figure 7b2,

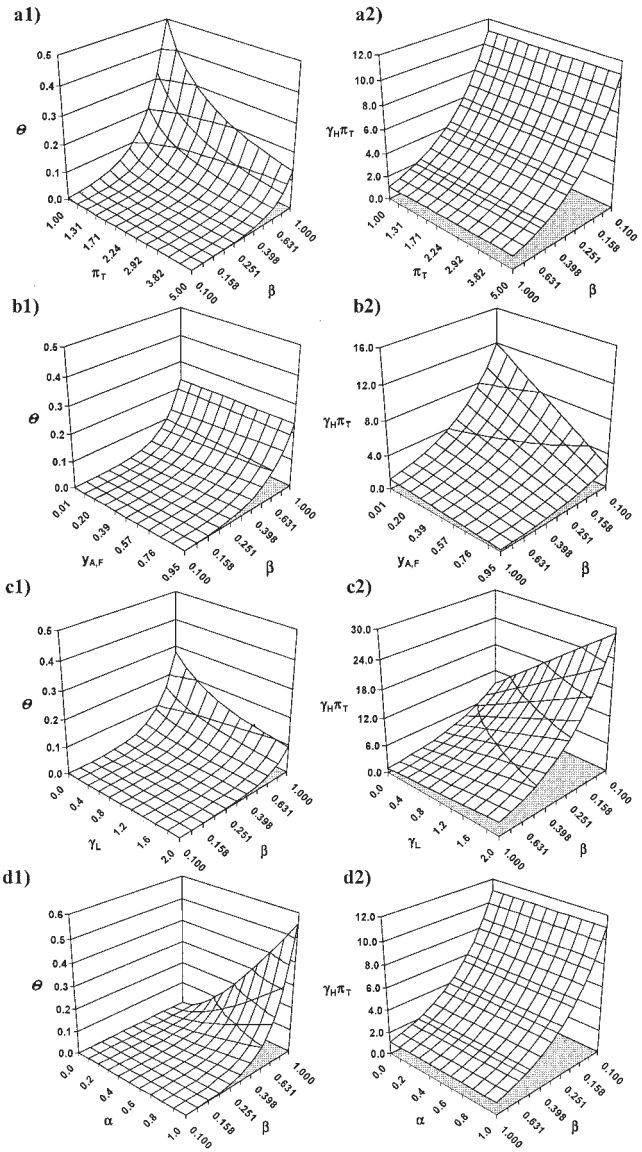

Figure 7. Effect on dimensionless throughput Θ on (a) π_T and β with $y_{A,F} = 0.1$, $\gamma_L = 0.2$ and $\alpha = 0.6$, (b) $y_{A,F}$ and β with $\pi_T = 2.0$, $\gamma_L = 0.2$ and $\alpha = 0.6$, (c) γ_L and β with $\pi_T = 2.0$, $y_{A,F} = 0.1$ and $\alpha = 0.6$, and (d) α and β with $\pi_T = 2.0$, $y_{A,F} = 0.1$ and $\gamma_L = 0.2$.

are very dramatic with $\gamma_H\pi_T$ increasing markedly as both $y_{A,F}$ and β decrease.

Clearly, this result is indicative of the corresponding increase in the desorption flow as these parameters both decrease. Figure 7d1 shows that as α and β both increase, Θ again essentially goes from a value of zero up to a value as high as 0.55 when $\alpha = \beta = 1.0$. In contrast $\gamma_H\pi_T$ is completely independent of α, but depends strongly on β, in the usual manner (Figure 7d2). As pure heavy component is always produced, it is not surprising that $\gamma_H\pi_T$, or equivalently R_H, does not depend on α, because α simply establishes where the heavy component concentration fronts are located in the column, which has nothing to do with the magnitudes of the recycle flows in a DR PSA cycle.

The negative effect of an increasing pressure ratio π_T on the dimensionless throughput Θ manifests through the $1/(1+\chi)$ term in Eq. 40 (also see Eq. 42). This result is a consequence of the fact that at a larger π_T, the pump, which has a given capacity, takes more time to transfer the gas from the column undergoing blowdown to the column undergoing pressurization. The positive effect of an increasing α on Θ is manifest through Eq. 42, and can be explained in two ways. With the size of the pump and, thus, u_F fixed, the amount of time it takes for the pump to switch the pressures between the columns is fixed, because only pure heavy component is being transported through it. So, with increasing α, the pump necessarily spends more time transferring gas during the constant pressure steps of the DR PSA cycle. In contrast, with the constant pressure step time Δt fixed, a larger α signifies a larger feed velocity u_F (thus, a larger capacity pump), and, therefore, a shorter pressure varying step time. In either case, the consequence is that a larger fraction of the total cycle time is associated with the constant pressure steps, which increases Θ through the effect of decreasing χ in Eq. 40.

The positive influence of a decreasing γ_L on Θ is directly associated with the marked effect it has on decreasing the desorption flow, as mentioned on numerous occasions above. The strong and consistently negative effect of an increasing selectivity (that is, smaller β) on Θ is manifest through Eq. 42, wherein a smaller β corresponds to a higher desorption flow that must be handled during the pressure varying steps; hence, Θ must decrease, because for a given pump, χ must increase. The lack of any effect of $y_{A,F}$ on Θ can be understood only be arguing that all the other effects are much more pronounced and tend to overwhelm the effect of $y_{A,F}$. This is in agreement with Eq. 43, which shows that the effect of $y_{A,F}$ decreases dramatically as β approaches unity, and, at the other extreme, when β approaches zero, the effect of $y_{A,F}$ (with it being restricted to values between zero and one) is dominated by γ_L.

It is worth making a few final remarks about the results presented in Figures 4 to 7. The ranges of the parameters investigated in this study are quite broad and generally reasonable. For example, the feed concentration $y_{A,F}$ ranges from 0.01 to 0.95, the selectivity β ranges from 0.1 to 1.0, the light product volumetric purge to feed ratio γ_L ranges from 0.01 to 2 (except when it is increased to 20 to show the extreme limit of $z_{\min}/L \rightarrow \alpha$ in Figure 6), the corresponding heavy product volumetric purge to feed ratio γ_H ranges from γ_L *to* 18.7 (with this maximum value obtained from the results in Figure 5c with $\pi_T = 1.5$, $y_{A,F} = 0.2$, $\gamma_L = 2.0$ and $\beta = 0.1$), the pressure ratio π_T ranges from 1 to 5, and α naturally ranges from 0 to 1.0. Recall that in all cases a binary feed is separated into two pure components with a 100% recovery of each component, which is truly remarkable when considering that the pressure ratio never exceeds five, and that this separation is still possible, at least based on isothermal, equilibrium theory, even with $\pi_T = 1.1$. What is equally remarkable is that the separation can be achieved for a wide range of feed concentrations $y_{A,F}$ and selectivities β, and it seems to be achievable no matter where the feed is located based on the position of α. However, depending on the actual values of some of these parameters, the throughput Θ can become exceedingly low, and the heavy product purge to feed ratio γ_H (or equivalently the heavy product recycle ratio R_H) can become exceedingly high. Nevertheless, these results surprisingly suggest that low selectivities and low-pressure ratios tend to maximize Θ, and minimize R_H, along with high feed concentrations and low light product volumetric purge to feed ratios, which are more obvious. However, these unusual trends are simply a consequence of the fact that the results in all cases are constrained to achieving perfect separation. In reality, these trends may not carry over to actual practice.

Conclusions

A new dual reflux (DR) PSA cycle that combines the essential features of a conventional (stripping reflux) PSA cycle with those of a relatively new enriching reflux PSA cycle, is analyzed to show its potential for separating gas mixtures into two relatively pure components at very high recoveries, with a minimal expenditure of energy. On the basis of isothermal equilibrium theory applied to a binary linear isotherm system, the ultimate separation is carried out where a binary feed is separated into two pure components with a 100% recovery of each component. An extensive parametric study, involving the feed concentration $y_{A,F}$ ranging from 0.01 to 0.95, the selectivity β ranging from 0.1 to 1.0, the light product volumetric purge to feed ratio γ_L ranging from 0.01 to 2, the corresponding heavy product volumetric purge to feed ratio γ_H ranging from γ_L to 19, the pressure ratio π_T ranging from 1 to 5, and α (an indicator of the feed location along the column) naturally ranging from 0 to 1.0, reveals that such an ultimate separation is indeed possible over a wide range of conditions and most surprisingly with pressure ratios never exceeding five and as low as 1.1.

However, in some cases, the throughput Θ can become very low, and the heavy product volumetric purge to feed ratio γ_H (or equivalently the heavy product recycle ratio R_H) can become very high, which is not desirable because large Θ and low γ_H are most probably necessary to make a DR PSA process economically viable. To circumvent this disconcerting result, this analysis suggests that, in order to both maximize Θ and minimize R_H, low-pressure ratios and low selectivities, along with high feed concentrations and low light product volumetric purge to feed ratios, should be used. The idea that very low-pressure ratios and less selective adsorbents may be advantageous to a DR PSA process for improving the performance is completely counterintuitive, yet intriguing. It is reasoned, however, that with the perfect separation constraint being imposed, these seemingly unusual trends are a natural and obvious consequence of the ideal analysis that may not carry over to actual practice. Nevertheless, this work clearly demonstrates the feasibility of a DR PSA cycle for carrying out the perfect separation of a binary gas mixture. However, because the model developed here is overly simplified and invalid under certain conditions, what remains to be proven is the extent to which such a separation can be achieved in practice, using only two DR PSA columns and a minimal expenditure of energy, as alluded to by this ideal analysis.

Acknowledgments

Financial support provided by MeadWestvaco, and the Separations Research Program at the University of Texas at Austin is greatly appreciated.

Notation

A_{cs} = cross sectional area of bed, m^2
k_i = Henry's law constant of species i, m^3 gas phase m^{-3} adsorbent
L = column length, m
n = total concentration of all species in the adsorbed phase, mol m^{-3} adsorbent
n_i = concentration of species i in the adsorbed phase, mol m^{-3} adsorbent
N_{Bl} = total moles of gas leaving the bed during the blowdown step, mol
N_F = total moles of gas fed to the bed during the feed step, mol
N_{HE} = total moles of gas leaving the heavy product end of the bed during the feed step, mol
N_{HF} = total moles of gas fed to the heavy product end of the bed during the purge step, mol
N_{HP} = total moles of gas leaving the PSA unit as heavy product during a half cycle, mol
N_{LE} = total moles of gas leaving the light product end of the bed during the purge step, mol
N_{LF} = total moles of gas fed to the light product end of the bed during the feed step, mol
N_{LP} = total moles of gas leaving the PSA unit as light product during a half cycle, mol
N_{Pr} = total moles of gas fed to the bed during the pressurization step, mol
P = total pressure, kg m^{-1} s^{-2}
P_H = purge step pressure, kg m^{-1} s^{-2}
P_L = feed step pressure, kg m^{-1} s^{-2}
P_i = partial pressure of species i, kg m^{-1} s^{-2}
P_{STP} = standard pressure, 101350 kg m^{-1} s^{-2}
R = ideal gas constant, 8.314 kg m^2 s^{-2} mol^{-1} K^{-1}
R_H = heavy product recycle ratio as defined in Eq. 20, dimensionless
R_L = light product recycle ratio as defined in Eq. 21, dimensionless
t = time, s
T_{STP} = standard temperature, 273.15 K
T = bed temperature, K
u = interstitial velocity, m s^{-1}
u_F = interstitial velocity of the feed stream, m s^{-1}
u_F^- = interstitial velocity of the gas right before the feed stream during the feed step, m s^{-1}
u_F^+ = interstitial velocity of the gas right after the feed stream during the feed step, m s^{-1}
u_{HE} = interstitial velocity of the gas leaving the heavy product end of the bed during the feed step, m s^{-1}
u_{HF} = interstitial velocity of the gas entering the heavy product end of the bed during the purge step, m s^{-1}
u_{LE} = interstitial velocity of the gas leaving the light product end during the feed step, m s^{-1}
u_{LF} = interstitial velocity of the gas entering the light product end during the feed step, m s^{-1}
u_{pump} = interstitial velocity of the gas just upstream of the pump, m s^{-1}
y_i = gas-phase mol fraction of species i, dimensionless
$y_{i,F}$ = gas-phase mol fraction of species i in the feed, dimensionless
z = distance from the top of the bed, m
z_a = location of characteristic a in Figure 3, m
z_b = location of characteristic b in Figure 3, m
z_F = location of feed, m
$z_{F,max}$ = maximum location for feed, m
$z_{F,min}$ = minimum location for feed, m
z_o = location of characteristic a and b at the beginning of blowdown in Figure 3, m

Greek letters

α = relative location of characteristic a from the bottom of the column at the beginning of the feed step as in Figure 3, dimensionless
β = selectivity of the adsorbent as defined in Eq. 8, dimensionless
β_i = selectivity of the adsorbent toward species i as defined in Eq. 5, dimensionless
χ = ratio of pressure varying step duration to constant pressure step duration, dimensionless.
ε = bed porosity, m^3 gas phase m^{-3} bed
γ_H = heavy product volumetric purge to feed ratio, dimensionless
γ_L = light product volumetric purge to feed ratio, dimensionless
ϕ = total moles of gas in the bed when saturated with pure heavy component at $P = P_L$, mol
π = ratio of bed pressures at different times during a pressure varying step, dimensionless
π_T = ratio of high to low pressures, dimensionless
θ = throughput as defined in Eq. 39, m^3 product gas kg^{-1} adsorbent s^{-1}
θ^* = characteristic throughput as defined by expression within brackets in Eq. 39, m^3 product gas kg^{-1} adsorbent s^{-1}
Θ = dimensionless throughput as defined in Eq. 38, dimensionless
ρ_s = apparent adsorbent density, kg m^{-3}
$\Delta\tau$ = time duration of a constant pressure step, dimensionless
$\Delta\tau_{max}$ = maximum time duration of a constant pressure step, dimensionless
Δt = time duration of a constant pressure step, s
Δt_{PV} = time duration of a pressure varying step, s

Subscripts

A = heavy component
B = light component
o = initial temporal condition of a characteristic during a step

Literature Cited

Diagne, D., M. Goto, and T. Hirose, "New PSA Process with Intermediate Feed Inlet Position and Operated with Dual Refluxes: Application to Carbon Dioxide Removal and Enrichment," *J. Chem. Eng. Japan*. **27**, 85 (1994).

Diagne, D., M. Goto, and T. Hirose, "Parametric Studies on CO_2 Separation and Recovery by Dual Reflux PSA Process Consisting of Both Rectifying and Stripping Sections," *Ind. Eng. Chem. Res.,* **34**, 3083 (1995).

Diagne, D., M. Goto, and T. Hirose, "Numerical Analysis of a Dual Refluxed PSA Process during Simultaneous Removal and Concentration of Carbon Dioxide Dilute Gas from Air," *J. Chem. Tech. Biotechnol.*, **65**, 29 (1996).

Ebner A. D., and J. A. Ritter, "Equilibrium Theory Analysis of Rectifying PSA for Heavy Component Production," *AIChE J*., **48** 1679 (2002).

McIntyre J. A., C. E. Holland, and J. A. Ritter, "High Enrichment and Recovery of Dilute Hydrocarbons by Dual-Reflux Pressure-Swing Adsorption," *Ind. Eng. Chem. Res*., **41** 3499 (2002).

McIntyre J. A., and J. A. Ritter, "Experimental Study of a Dual-Reflux Pressure-Swing Adsorption Cycle for Gas Separation," *Ind. Eng. Chem. Res*., in press (2005).

Knaebel K. S., and F. B. Hill, "Pressure Swing Adsorption: Development of an Equilibrium Theory for Gas Separations," *Chem. Eng. Sci.,* **40,** 2351 (1985).

Ruthven, D. M., S. Farooq, and K. S. Knaebel, *Pressure Swing Adsorption*, VCH, New York (1994).

Subramanian D., and J. A. Ritter, "Equilibrium Theory for Solvent Vapor Recovery by Pressure Swing Adsorption: Analytical Solution for Process Performance," *Chem. Eng. Sci.*, **52**, 3147 (1997).

Yoshida M., J. A. Ritter, A. Kodama, M. Goto, and T. Hirose, "Enriching Reflux and Parallel Equalization-PSA Process for Concentrating Trace Components in Air," *Ind. Eng. Chem. Res.*, **42**, 1795 (2003).

Manuscript received April 29, 2003, and revision received Jan. 6, 2004.